dominately TTN in character. These two HOMO's, from which one and two electrons are removed to form the mono- and dications, tri- and tetracations have $a_u(\pi,XZ_-)$ and $b_{3g}(\pi,YZ_+)$ symmetry representations, respectively.[8c]

We conclude, therefore, that upon successive reversible oxidations, the electrons are being removed from molecular orbitals which are largely localized on the TTN ligand with each square-planar platinum atom maintaining a "formal charge" of $+2(d^8)$ in each species. In other words, the "formal charge" on the TTN ligand decreases from $-4 \rightarrow -3 \rightarrow -2 \rightarrow -1 \rightarrow 0$ as n in $[TTNPt_2(PPh_3)_4]^n$ increases from $0 \rightarrow +1 \rightarrow +2 \rightarrow +3 \rightarrow +4$ (each sulfur atom remains a two-electron donor). The representative limiting valence-bond structures of these five species are summarized below.

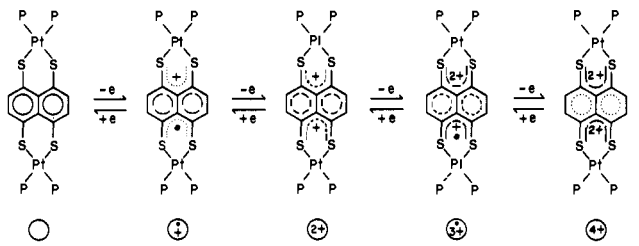

We believe that **1** represents the first metal "tetrathiolene" complex which spans five reversible oxidation states. Attempts to synthesize and explore the stereochemical as well as electronic structure of other metal tetrathiolenes are in progress.

Acknowledgments. We thank M. L. Kaplan, F. C. Schilling, and B. E. Prescott for technical assistance.

References and Notes

(1) For the nomenclature of "metal dithiolenes", see the excellent review by G. N. Schrauzer, *Acc. Chem. Res.*, **2**, 72 (1969).
(2) For the preparation of TTN ($C_{10}H_4S_4$, dehydrotetrathianaphthazarin, naphtho[1,8-*cd*:4,5-*c'd'*]bis[1,2]dithiole), see F. Wudl, B. Miller, and D. E. Schaffer, *J. Am. Chem. Soc.*, **98**, 252 (1976).
(3) The corresponding bands in free TTN[2] occur at 1540 (s), 1362 (s), 1185 (vs), and 797 (vs) cm^{-1}. The 1172-cm^{-1} band, however, interferes with two very weak bands of triphenylphosphine at 1160 and 1182 cm^{-1}.
(4) These potentials can be transformed to the corresponding SCE values by adding a factor of 0.285 V.
(5) See, for example, J. B. Headrige, "Electrochemical Techniques for Inorganic Chemists", Academic Press, New York, N.Y., 1969, Chapter 5.
(6) (a) A. Y. Girgis, Y. S. Sohn, and A. L. Balch, *Inorg. Chem.*, **14**, 2327 (1975); (b) F. C. Senftleber and W. E. Beiger, Jr., *J. Am. Chem. Soc.*, **97**, 5018 (1975); (c) A. Davison, N. Edelstein, R. H. Holm, and A. H. Maki, *ibid.*, **85**, 2029 (1963).
(7) (a) We expect a 1:4:1 triplet and a 1:8:18:8:1 quintet for the hyperfine interaction(s) with one and two platinum (natural abundance: 33.4% ^{195}Pt with $I = \frac{1}{2}$) atoms, respectively. (b) Other possibilities include ion-pairing or electron transfer/exchange mechanisms (cf. A. Carrington and A. D. McLachlan, "Introduction to Magnetic Resonance", Harper and Row, New York, N.Y., 1967, pp 215–217).
(8) (a) B. K. Teo, M. B. Hall, R. F. Fenske, and L. F. Dahl, *Inorg. Chem.*, **14**, 3103 (1975); (b) M. B. Hall and R. F. Fenske, *ibid.*, **11**, 768 (1972). (c) The *z* and *y* axes of the metal atoms were chosen to be perpendicular to the molecular plane and bisecting the P–M–P angles, respectively.

Boon-Keng Teo,* F. Wudl, J. H. Marshall, A. Kruger
Bell Laboratories
Murray Hill, New Jersey 07974
Received December 6, 1976

Synthesis and Electronic Properties of the Tetranuclear Trianions $[Fe_4S_4(SR)_4]^{3-}$, Analogues of the 4-Fe Active Sites of Reduced Ferredoxins

Sir:

The lower molecular weight iron-sulfur redox proteins[1] contain three recognized types of active sites, $[Fe(S\text{-}Cys)_4]^{-,2-}$, $[Fe_2S_2(S\text{-}Cys)_4]^{2-,3-}$, and $[Fe_4S_4(S\text{-}Cys)_4]^{-,2-,3-}$, which function in the indicated total oxidation

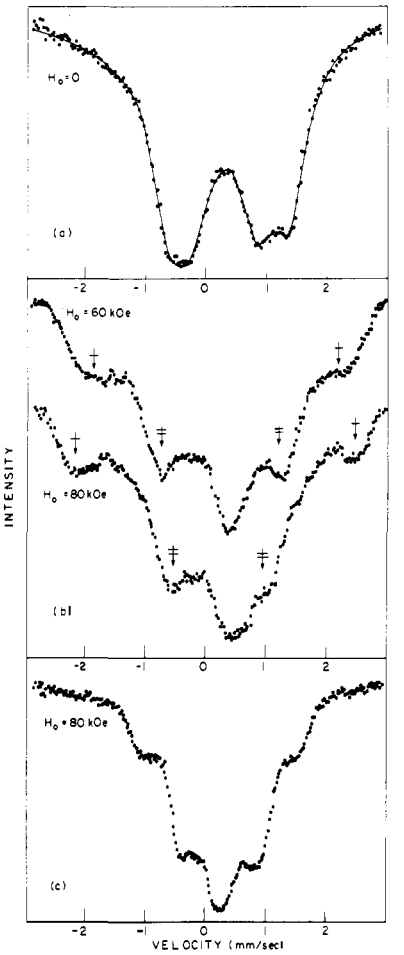

Figure 1. Mössbauer spectra at 4.2 K. (a) $(Et_4N)_3[Fe_4S_4(SPh)_4]$ (I) at $H_0 = 0$. The solid line is a least-squares fit, assuming two sites, Lorentzian line shapes, and line intensities, positions, and widths as free parameters, and gives the $\Delta E_{1,2}$, $\delta_{1,2}$ data in Table I. (b) I at $H_0 = 60$ and 80 kOe; ∓ and ∓ designate lines moving apart and moving together, respectively, with increasing H_0. (c) $(Et_4N)_3[Fe_4S_4(SCH_2Ph)_4]$ (III) at $H_0 = 80$ kOe.

levels. A prime goal of the synthetic analogue approach[2] to elucidation of key properties of these sites is preparation and isolation in substance of analogues of each of the seven site species. Four such analogues, $[Fe(SR)_4]^{-,2-}$, $[Fe_2S_2(SR)_4]^{2-}$, and $[Fe_4S_4(SR)_4]^{2-}$, have previously been obtained.[2,3] Here we report isolation of a fifth synthetic species, $[Fe_4S_4(SR)_4]^{3-}$, previously accessible only by generation in solution[4,5] and analogous to the 4-Fe sites of reduced ferredoxins (Fd_{red}).

Under *rigorously* anaerobic anhydrous conditions a solution containing $(Et_4N)_2[Fe_4S_4(SPh)_4]$[4] (6.5 mmol), Et_4NCl (6.5 mmol), and sodium acenaphthylenide (8.2 mmol) in 100 mL of freshly distilled hexamethylphosphoramide was stirred for 5 h. Product precipitation with THF followed by recrystallization from acetonitrile–THF afforded pure $(Et_4N)_3[Fe_4S_4(SPh)_4]$ (I) (85%).[6] Similar procedures but with $(R_4N)(BPh_4)$ as common cation source yielded $(Me_4N)_3[Fe_4S_4(SPh)_4]$ (II) and $(Et_4N)_3[Fe_4S_4(SCH_2Ph)_4]$ (III) (65–85%).[6] All three salts are intensely oxygen-sensitive,[7] black crystalline solids. Also obtained by this procedure is the highly crystalline salt $(Et_3NMe)_3[Fe_4S_4(SPh)_4]$, currently under structural investigation.[8]

The isoelectronic relationship $[Fe_4S_4(SR)_4]^{3-} \equiv Fd_{red}$, previously asserted from generated trianion–protein comparative properties,[5] is fully confirmed with isolated analogues. Absorption spectra are slightly better resolved and $[Fe_4S_4(SCH_2Ph)_4]^{3-}$ (λ_{max} 358 nm, ϵ 17 600) shows diminished visible absorption vs. $[Fe_4S_4(SCH_2Ph)_4]^{2-}$, characteristic of the Fd_{ox}/Fd_{red} transition.[1,9] Axial EPR spectra are

Table I. Mössbauer Data for Reduced Analogues and Proteins

	T, °K	ΔE_1 (mm/s)	δ_1 (mm/s)[a]	ΔE_2 (mm/s)	δ_2 (mm/s)[a]	Ref
$(Et_4N)_3[Fe_4S_4(SPh)_4]$ (I)	77	1.43 ± 0.05	0.47 ± 0.03	0.86 ± 0.05	0.44 ± 0.03	
	4.2	1.96	0.50	1.09	0.40	This work[c]
$(Me_4N)_3[Fe_4S_4(SPh)_4]$ (II)	77	0.91	0.52	0.74	0.38	
	4.2	1.80	0.52	1.03	0.38	This work[c]
$(Et_4N)_3[Fe_4S_4(SCH_2Ph)_4]$ (III)	77	1.0	0.44			
	4.2	1.45	0.48	0.94	0.49	This work[c]
C. pasteurianum 8-Fe Fd_{red} (IV)	77	1.25	0.57[b]			
	4.2	1.54	0.58[b]			10, 15
B. stearothermophilus 4-Fe Fd_{red} (V)	77	1.82	0.60[b]	1.18	0.50[b]	11

Referenced to metallic iron [a] at the same temperature, [b] at room temperature. [c] Measured using a ^{57}Co in Rh source.

observed in frozen acetonitrile solutions with $g_\parallel, g_\perp = 2.04, 1.93$ (R = CH_2Ph) and 2.06, 1.93 (R = Ph). Native Fd_{red} spectra are rhombic[1,10-14] (e.g., $g = 1.88, 1.92, 2.06$[10]) but convert to axial shapes when proteins are unfolded in 80% Me_2SO/H_2O[13,14] (e.g., $g_\parallel = 2.06$, $g_\perp = 1.94$[14]). Trianion spectra are best observed at $\lesssim$15 K and, as with Fd_{red}, rapidly decrease in intensity at higher temperatures indicating similar relaxation mechanisms.

Isolated trianion salts permit the first detailed study of magnetic properties of this oxidation level and provide better resolved ^{57}Fe Mössbauer spectra free of dianion impurities.[5] Measurements of I with a SQUID-type susceptometer at 4.2–338 K yield continually increasing magnetic moments μ_t per tetramer: 2.05, 4.2; 3.43, 150; 4.35, 299; 4.54 μ_B, 338 K. These results confirm a spin-doublet ground state and establish antiferromagnetic interactions within the Fe_4S_4 core, suspected for Fd_{red} from the temperature dependencies of cysteinyl methylene ^1H shifts[15] and detected in low temperature Mössbauer spectra.[16] Deviation of $\mu_t = 2.05\ \mu_B$ (4.2 K) from the doublet state moment (1.71 μ_B) calculated from g values reflects a paramagnetic impurity and/or occupation of higher spin levels. Mössbauer spectra of I–III (Table I) in zero field consist of at least two overlapping doublets with temperature invariant isomer shifts δ but temperature dependent quadrupole splittings ΔE. Isomer shifts are larger than for the corresponding dianions,[5,17] indicative of greater Fe(II) core character as reflected by the formal 3Fe(II) + Fe(III) core description. Assuming two iron subsites per core the fitting procedure of Figure 1a yields an approximate 1:1 integrated intensity for the two doublets of I and II. However, broadened spectral lines at 4.2 K compared to 77 K indicate the possible onset of magnetic hyperfine interactions owing to slow electronic spin relaxation. The spectrum of I in external fields $H_0 < 40$ kOe is broadened and at $40 \leq H_0 \leq 80$ kOe (Figure 1b) contains two pairs of resolved lines flanking a central unresolved absorption. One pair exhibits an increasing and the other a decreasing splitting with increasing H_0, indicating at least two magnetically inequivalent subsites with positive and negative hyperfine fields, respectively. The magnitudes of the splittings depend on the terminal ligand, with that for $[Fe_4S_4(SCH_2Ph)_4]^{3-} \sim 50\%$ smaller than for $[Fe_4S_4(SPh)_4]^{3-}$ (Figure 1c). In both cases magnetic fields at the iron nuclei are different than H_0, consistent with a spin-doublet ground state and attendant magnetic hyperfine structure arising from unpaired spin density at the iron subsites. Moreover, the magnetic hyperfine interaction constants estimated from the observed splittings are different for the subsites, implying different spin densities at each. In addition to the different magnitudes and directions of the magnetic hyperfine interactions in the subsites, different quadrupole interactions, randomization in the powder sample of the angle between the principal component of the electric field gradient and the magnetic hyperfine field, and possible asymmetries in both the quadrupole interaction and magnetic hyperfine interaction contribute to the overall complexity of the spectra.

The Mössbauer spectral features of $[Fe_4S_4(SR)_4]^{3-}$ are comparable with those of several Fd_{red} proteins[11,12,16] (Table I). In IV the presence of more than one subsite is suggested by broadened absorption line widths whereas in V two such sites within a *single* core are clearly resolved with δ and ΔE values fairly close to those for $[Fe_4S_4(SPh)_4]^{3-}$. Application of large external magnetic fields to both proteins affords two overlapping magnetic spectra with different magnitudes and opposite signs of magnetic hyperfine interactions,[12,16] again consistent with present observations and a qualitative model of the electronic structure of Fd_{red} presented elsewhere.[18] The close correspondence between Fd_{red} and its synthetic analogues indicates that iron subsite inequivalence in $[Fe_4S_4(SR)_4]^{3-}$ clusters is an intrinsic property and is only secondarily influenced by protein structure and environment, which may serve to enhance or diminish this effect. In contrast, there is detectable only a slight subsite inequivalence in 4-Fe Fd_{ox} clusters[16] and none whatever in their $[Fe_4S_4(SR)_4]^{2-}$ analogues.[2,17,19] Details of the synthesis and electronic and reactivity properties of $[Fe_4S_4(SR)_4]^{3-}$ complexes will be presented in subsequent reports.

Acknowledgment. This research was supported by National Institutes of Health Grants GM-22351 and GM-22352 at Stanford University and at the Francis Bitter National Magnet Laboratory, M.I.T., by the National Science Foundation. G.C.P. was partially supported by an NIH Biomedical Sciences Support Grant administered by M.I.T.

References and Notes

(1) W. H. Orme-Johnson, *Annu. Rev. Biochem.*, **43**, 159 (1973); G. Palmer in "The Enzymes", Vol. XII, 3rd ed, Part B, P. D. Boyer, Ed., Academic Press, New York, N.Y., 1975, pp 1–56.
(2) For reviews cf. R. H. Holm *Endeavour*, **34**, 38 (1975); R. H. Holm and J. A. Ibers in "Iron-Sulfur Prteins", Vol. III, W. Lovenberg, Ed., Academic Press, New York, N.Y., 1977, Chapter 7.
(3) R. W. Lane, J. A. Ibers, R. B. Frankel, and R. H. Holm, *Proc. Natl. Acad. Sci. U.S.A.*, **72**, 2868 (1975); R. W. Lane, J. A. ibers, R. B. Frankel, G. C. Papaefthymiou, and R. H. Holm, *J. Am. Chem. Soc.*, **99**, 84 (1977); see also D. Coucouvanis, D. Swenson, N. C. Baenziger, D. G. Holah, A. Kostikas, A. Simopoulos, and V. Petrouleas, *ibid.*, **98**, 5721 (1976).
(4) B. V. DePamphilis, B. A. Averill, T. Herskovitz, L. Que, Jr., and R. H. Holm, *J. Am. Chem. Soc.*, **96**, 4159 (1974).
(5) R. B. Frankel, T. Herskovitz, B. A. Averill, R. H. Holm, P. J. Krusic, and W. D. Phillips, *Biochem. Biophys. Res. Commun.*, **58**, 974 (1974).
(6) Anal. Calcd for $C_{48}H_{80}N_3S_8Fe_4$: C, 48.89; H, 6.84; N, 3.56; S, 21.76; Fe, 18.95. Found: C, 48.79; H, 6.79; N, 3.75; S, 21.64; Fe, 18.75. Other new compounds also gave satisfactory elemental analyses.
(7) As testified by $E_{1/2}$ values (vs. SCE) for $[Fe_4S_4(SR)_4]^{2-,3-,4-}$ −1.04 (R = Ph), −1.25 V (R = CH_2Ph).
(8) J. Renaud, R. H. Holm, and J. A. Ibers, research in progress.
(9) S. G. Mayhew, D. Peterling, G. Palmer, and G. P. Foust, *J. Biol. Chem.*, **244**, 2830 (1969); K. Uyeda and J. C. Rabinowitz, *ibid.*, **246**, 3111 (1971).
(10) N. A. Stombaugh, R. H. Burris, and W. H. Orme-Johnson, *J. Biol. Chem.*, **248**, 7951 (1973).
(11) K. Gersonde, H.-E. Schlaak, M. Breitenbach, F. Parak, H. Eicher, W. Zgorzalla, M. G. Kalvius, and A. Mayer, *Eur. J. Biochem.*, **43**, 307 (1974).
(12) R. N. Mullinger, R. Cammack, K. K. Rao, D. O. Hall, D. P. E. Dickson, C. E.

Johnson, J. D. Rush, and A. Simopoulos, *Biochem. J.*, **151**, 75 (1975).
(13) R. Cammack, *Biochem. Soc. Trans.*, **3**, 482 (1975).
(14) R. E. Anderson, G. Anger, L. Petersson, A. Ehrenberg, R. Cammack, D. O. Hall, R. Mullinger, and K. K. Rao, *Biochim. Biophys. Acta*, **376**, 63 (1975).
(15) W. D. Phillips, C. C. McDonald, N. A. Stombaugh, and W. H. Orme-Johnson, *Proc. Natl. Acad. Sci. U.S.A.*, **71**, 140 (1974).
(16) C. L. Thompson, C. E. Johnson, D. P. E. Dickson, R. Cammack, D. O. Hall, U. Weser, and K. K. Rao, *Biochem. J.*, **139**, 97 (1974).
(17) δ (mm/s), 4.2 K $[Fe_4S_4(SPh)_4]^{2-}$, 0.35; $[Fe_4S_4(SCH_2Ph)_4]^{2-}$, 0.34: R. B. Frankel, B. A. Averill, and R. H. Holm, *J. Phys. (Paris)*, **35**, C6-107 (1974).
(18) D. P. E. Dickson, C. E. Johnson, C. L. Thompson, R. Cammack, M. C. W. Evans, D. O. Hall, K. K. Rao, and U. Weser, *J. Phys. (Paris)*, **35**, C6-343 (1974); R. Cammack, D. P. E. Dickson, and C. E. Johnson in "Iron-Sulfur Proteins", Vol. III, W. Lovenberg, Ed., Academic Press, New York, N.Y., 1977, Chapter 8.
(19) R. H. Holm, B. A. Averill, T. Herskovitz, R. B. Frankel, H. B. Gray, O. Siiman, and F. J. Grunthaner, *J. Am. Chem. Soc.*, **96**, 2644 (1974).
(20) Visiting Scholar, 1975–1976; Department of Chemistry, La Trobe University, Bundoora, Victoria, Australia.

R. W. Lane, A. G. Wedd,[20] W. O. Gillum
E. J. Laskowski, R. H. Holm*
Department of Chemistry, Stanford University
Stanford, California 94305

R. B. Frankel,* G. C. Papaefthymiou
Francis Bitter National Magnet Laboratory
Massachusetts Institute of Technology
Cambridge, Massachusetts 02139

Received November 15, 1976

Nuclear Analogues of β-Lactam Antibiotics. 1. The Total Synthesis of a 7-Oxo-1,3-diazabicyclo[3.2.0]heptane-2-carboxylic Acid via a Versatile Monocyclic β-Lactam Intermediate

Sir:

The search for more effective antibacterial agents has led to the partial synthesis of a vast number of penicillin and cephalosporin derivatives which differ primarily in the nature of the acylamino substituent at C-6(7) and, for cephalosporins, the substituent at C-3. Analogous structures with more profound modifications, particularly new ring systems, are of considerable interest because they have the potential of offering improved therapy and may be useful in determining the mechanism of action of the β-lactam class of antibiotics. Only a limited number of such nuclear analogues are known because the preparation of each requires either extensive degradation and resynthesis starting from the natural products[1] or a multistep total synthesis.[2] We have developed a versatile monocyclic β-lactam intermediate[3] which allows for the synthesis of a wide variety of biologically active nuclear analogues.[4] The stereoselective synthesis of this key intermediate (**1**) and its subsequent conversion to a bicyclic structure (**2**) which incorporates some important features of the penicillins is the subject of this communication.

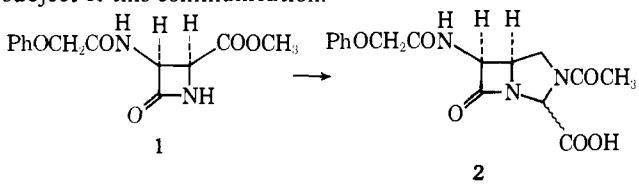

1 **2**

Addition of the mixed anhydride of azidoacetic acid and trifluoracetic anhydride[5] to a mixture of triethylamine and the imine formed from 2,4-dimethoxybenzylamine and methyl glyoxylate afforded *cis*-azido-β-lactam **3**[6] (58%; mp 82–84 °C; λ_{max}^{Nujol} 4.72 (azide) and 5.62 μ (β-lactam CO); $\delta_{Me_4Si}^{CDCl_3}$ 4.08 and 4.68 (d, J = 5.5 Hz, β-lactam C-H's)) with none of the trans isomer detected. The conversion of azide **3** into

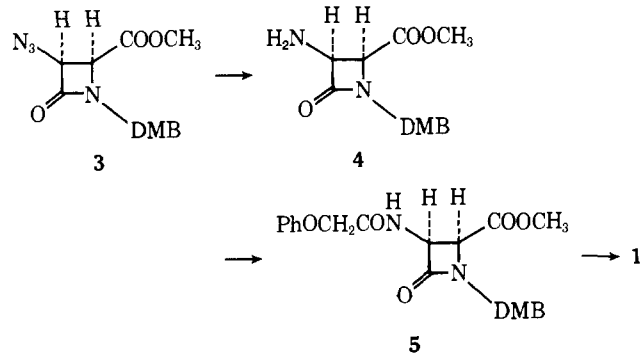

3 **4** **5**

phenoxyacetylamide **1** was accomplished in the following manner.

Catalytic hydrogenation of azide **3** (10% Pd-C, EtOH, 60 psi, 40 °C, 2 h) afforded the amine **4** as a clear gum which was acylated with phenoxyacetyl chloride[7] (Et_3N, CH_2Cl_2, 0 °C, 1 h) to give amide **5** in 84% yield for the two steps. The β-lactam nitrogen was conveniently deblocked by oxidative cleavage with buffered potassium persulfate[8] (4 equiv of $K_2S_2O_8$, 2 equiv of $Na_2HPO_4 \cdot 7H_2O$, 40% aqueous CH_3CN, reflux, 1 h) to afford phenoxyacetylamide **1** [(69%; mp 140–141 °C; λ_{max}^{Nujol} 5.63, 5.73, and 6.00 μ; $\delta_{Me_4Si}^{Me_2SO\text{-}d_6}$ $CDCl_3$ 3.59 (s, $COOCH_3$), 4.35 (d, J = 6 Hz, C-2H), 4.48 (s, $PhOCH_2CO$–), 5.33 and 5.50 ((d, J = 6 Hz, C-3H) also split by C-3 NH (d, J = 10 Hz)); *m/e* 278 (M^+) and 235 ($M^+ - 43$))].

Intermediate **1** is well suited for conversion into a variety of β-lactam antibiotic nuclear analogues which possess structural features believed necessary for good antibacterial activity.[9] The 7-oxo-1,3-diazabicyclo[3.2.0]heptane-2-carboxylic acid system **2**, a penicillin nuclear analogue, was selected as an initital synthetic target.

Selective sodium borohydride reduction[10] of the methyl ester of **1** afforded alcohol **6** (79%; H_2O-THF, 0 °C, 1 h) which was converted into the tosylate derivative (**7**) (79%; *p*-TsCl, pyr, 0 °C). Sodium iodide displacement gave iodide **8** (85%; NaI, acetone, reflux, 6 h) which was subsequently displaced with azide ion to yield azide **9** (75%; NaN_3, DMF, 25 °C, 48 h). Catalytic hydrogenation of **9** (10% Pd-C, EtOH, 25 °C, 2 h) followed by condensation of the resulting amine (**10**) with benzyl glyoxylate ($MgSO_4$, CH_2Cl_2, 25 °C, 2 h) afforded crystalline imine **11** (65%; mp 129–131 °C; λ_{max}^{Nujol} 5.62, 5.69, and 6.01 μ; $\delta_{Me_4Si}^{CDCl_3}$ 3.65 (m, $-CH_2N{=}CH$), 4.05 (m, C-2H), 4.45 (s, OCH_2CO), 5.20 (s, $COOCH_2Ph$), 5.36 and 5.52 (s, J = 5.5 Hz, C-3H coupled to C-2H and CONH), and 8.00 (d, J = 9 Hz, CH_2CONH); *m/e* 395 (M^+), 304, 260, 217). Treatment of **11** with acetyl chloride (CH_2Cl_2, pyr, 0 to 25 °C, 2 h) resulted in acylative cyclization to give benzyl ester **12** (mp 148–150 °C; λ_{max}^{Nujol} 5.57, 5.75, 5.96, and 6.15 μ; $\delta_{Me_4Si}^{CDCl_3}$ 1.93 (s, $COCH_3$), 4.52 (s, $PhOCH_2CO$), 5.15 (s, $COOCH_2Ph$), 5.40 (m, C-6H), and 5.93 (s, C-2H); *m/e* 437 (M^+), 302, 274, 247, 232, 205, 69) in 16–20% yield after purification by either column chromatography or fractional crystallization. ^1H NMR spectral evidence indicated that **12**

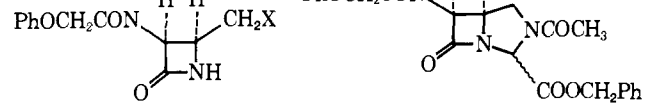

6, X = OH
7, X = OTs
8, X = I
9, X = N_3
10, X = NH_2
11, X = N=$CHCO_2CH_2Ph$

12